

# Determination of the Phonon Spectrum from Coherent Neutron Scattering by Polycrystals\*

N. Breuer

Institut für Festkörperforschung der Kernforschungsanlage Jülich, Jülich,  
 Fed. Rep. Germany

Received August 26, 1974

*Abstract.* As proposed by Bredov *et al.* [2, 3] the phonon spectrum can be obtained approximately from coherent neutron scattering by polycrystals if suitable averages over scattering angles are considered. The accuracy of this method is estimated by comparison with analytical results for simple lattice models (discussed here in particular for Aluminium). The errors are about 5% for low order moments and about 50% near van Hove singularities for “cold” neutrons (wavelength of the order of the nearest-neighbour-distance).

## 1. Introduction

In Bravais lattices the phonon spectrum is given by:

$$g(\varepsilon) = 1/3V \cdot \sum_{\sigma=1}^3 \int_V d\mathbf{q} \delta(\varepsilon - \hbar\omega^\sigma(\mathbf{q})) \quad (1)$$

$\mathbf{q}$ ,  $\sigma$ ,  $\hbar\omega^\sigma(\mathbf{q})$ : phonon wave vector, polarization, energy  
 $V$ : volume of the Brillouin zone (BZ).

The spectrum can be obtained by neutron scattering in two ways [4]:

- a) from coherently scattering single crystals one obtains  $\omega^\sigma(\mathbf{q})$  and then determines  $g$  via (1),
- b) incoherent scattering by single or polycrystals gives  $g$  directly.

For coherently scattering polycrystals neither method can be applied. Bredov *et al.* [2] and Oskotskii [3], however, proposed a method to obtain  $g$  approximately in this case; the main idea is to average over scattering angles for fixed energy transfer (Sections 3 and 4). Bredov's approximation has been used variously [2, 5], but its validity still remained unclear [6]. In this paper we check its accuracy by comparison

with analytical results obtained from simple lattice models; in particular we compare:

- a)  $g(\varepsilon)$  near fixed  $\varepsilon$  defined by van Hove singularities
- b) integral properties of  $g$ , e.g.  $\langle \varepsilon^2 \rangle = \int d\varepsilon g(\varepsilon) \varepsilon^2$ .

## 2. One-Phonon-Absorption Cross Section

In standard neutron scattering theory the differential one-phonon-absorption cross section\*\* for scattering by a single crystal at temperature  $T$ , containing  $N$  atoms of mass  $M$ , is [4]\*\*\* (see Fig. 1):

$$K = \frac{d^2\sigma}{d\varepsilon d\Omega} = C(\varepsilon, k_0, T) I(\boldsymbol{\kappa}, \varepsilon) \quad (2)$$

$$I(\boldsymbol{\kappa}, \varepsilon) = 8\pi k k_0 \sum_{\sigma=1}^3 \int d\mathbf{q} \delta(\varepsilon - \hbar\omega^\sigma(\mathbf{q})) \cdot \delta(\boldsymbol{\kappa} - \mathbf{q}) (\mathbf{q} \cdot \mathbf{e}^\sigma(\mathbf{q}))^2 \cdot F(\mathbf{q})$$

\*\* Without loss of generality only phonon absorption ( $\varepsilon > 0$ ) is considered.

\*\*\* For convenience we did not employ the standard notation

$$K = N \frac{\sigma_c}{4\pi} \cdot \frac{k}{k_0} \cdot \frac{1}{\hbar} \cdot S_{\text{coh}}^1 \left( \boldsymbol{\kappa}, \omega = \frac{\varepsilon}{\hbar} \right);$$

$\sigma_c = 4\pi a_c^2$ ;  $S_{\text{coh}}^1$ : “scattering law” for one phonon absorption.

\* This paper is a condensed version of the report [1], Berichte der Kernforschungsanlage Jülich – Nr. 1035-FF (71 pages), available from: Zentralbibliothek der Kernforschungsanlage Jülich GmbH, D-5170 Jülich 1 (Fed. Rep. Germany), Postfach 365.

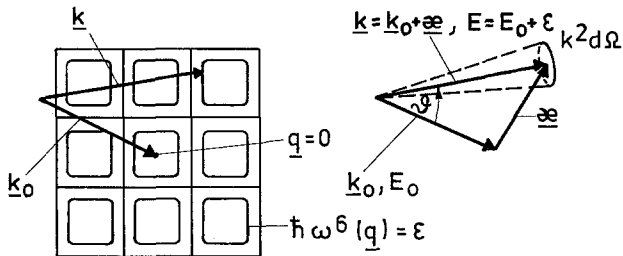


Fig. 1. Coherent scattering by a single crystal (rec. space); incoming neutron: mass  $m$ , wave vector  $\mathbf{k}_0$ , energy  $E_0$ ; outgoing neutron: mass  $m$ , wave vector  $\mathbf{k}$ , energy  $E$ ;  $\hbar \boldsymbol{\kappa} = \hbar(\mathbf{k} - \mathbf{k}_0)$ : momentum transfer;  $\varepsilon = E - E_0$ : energy transfer;  $\vartheta$ : scattering angle,  $d\Omega$ : solid angle for outgoing neutron

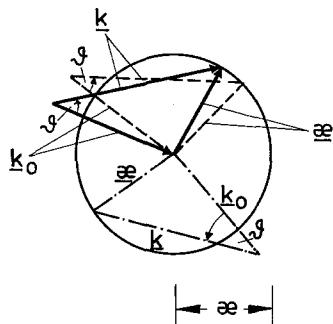


Fig. 2. The polycrystalline cross section for fixed  $\vartheta$  is obtained by averaging over all directions of  $\boldsymbol{\kappa}$

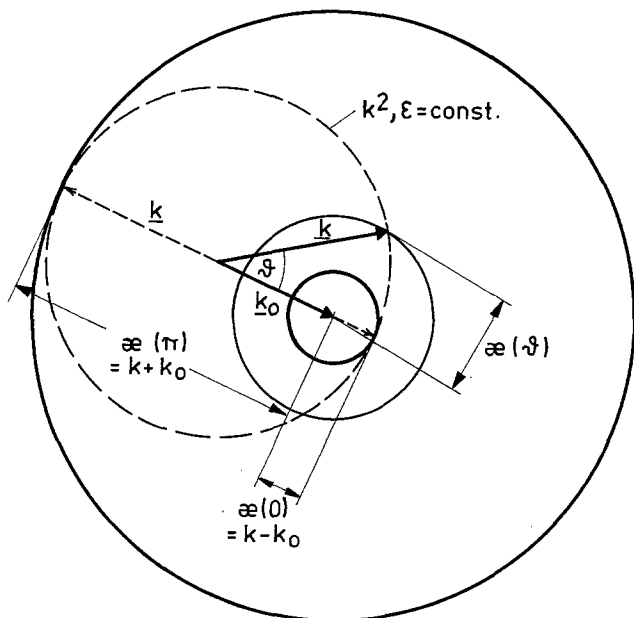


Fig. 3.  $\vartheta$ -dependence of  $\kappa(\vartheta)$  for fixed  $\varepsilon$

$$C(\varepsilon, k_0, T) = N a_c^2 \hbar^2 / (16 \pi M k_0^2) \cdot 1 / (\exp(\varepsilon/kT) - 1)$$

$\mathbf{e}^\sigma(\mathbf{q})$ : polarization vector,  $F(\mathbf{q})$ : Debye-Waller factor (DWF),  $a_c$ : coherent scattering length.

Scattering takes place if  $\boldsymbol{\kappa}$  is located on a constant phonon energy surface in reciprocal lattice,  $\hbar \omega^\sigma(\mathbf{q}) = \varepsilon$ , and if  $(\boldsymbol{\kappa} \cdot \mathbf{e}^\sigma(\boldsymbol{\kappa})) \neq 0$ . The polycrystalline cross section is obtained by averaging (2) over all rotations of the rigid scattering triangle  $(\mathbf{k}_0, \boldsymbol{\kappa}, \mathbf{k})$  (fixed  $\vartheta, \varepsilon$ , Fig. 2), i.e. averaging over all directions of  $\boldsymbol{\kappa}$ :

$$\bar{\delta} = 1/4\pi \cdot \int d\Omega_{\boldsymbol{\kappa}} \delta(\boldsymbol{\kappa} - \mathbf{q}) = 1/2\pi q \cdot \delta(\kappa^2 - q^2)$$

and

$$\bar{K} = C \cdot \bar{I}(\kappa, \varepsilon) = C \sum_{\sigma} \int d\mathbf{q} \delta(\varepsilon - \hbar \omega^\sigma(\mathbf{q})) \cdot (\mathbf{q} \cdot \mathbf{e}^\sigma(\mathbf{q}))^2 \cdot (1/q) 4k k_0 \delta(\kappa^2 - q^2) F(\mathbf{q}). \quad (3)$$

One gets scattered intensity from those points of the reciprocal lattice, where the spherical surface of radius  $\kappa$  intersects  $\hbar \omega^\sigma(\mathbf{q}) = \varepsilon$ ; for given  $\mathbf{k}_0$  and  $\varepsilon$  there is a one-to-one correspondence between  $\kappa$  and the scattering angle  $\vartheta$ :  $\kappa^2 = k_0^2 + k^2 - 2k k_0 \cos \vartheta$ , i.e. with increasing  $\vartheta$  the radius of the sphere increases from  $\kappa = k - k_0$  (forward scattering) to  $\kappa = k + k_0$  (back scattering,  $\vartheta = \pi$ ) (Fig. 3).

### 3. Average over Scattering Angles

To obtain  $\bar{g}$  one has to cover at least one whole BZ which is not possible for one  $\vartheta$ ; therefore one must vary  $\vartheta$ . The simplest method, which also is used experimentally [5], is to integrate over all  $\vartheta$  with equal weight equivalent to averaging over  $\vartheta$ ,  $1/2 \cdot \int_{-1}^{+1} d(\cos \vartheta) \dots$ , resulting in

$$\bar{K} = C \bar{I} = C \sum_{\sigma} \int d\mathbf{q} \delta(\varepsilon - \hbar \omega^\sigma(\mathbf{q})) \cdot G^\sigma(\mathbf{q}) \quad (4)$$

$$G^\sigma(\mathbf{q}) = F(\mathbf{q}) \cdot (\mathbf{q} \cdot \mathbf{e}^\sigma(\mathbf{q}))^2 / q \cdot \Theta_q,$$

$$\Theta_q = \begin{cases} 1 & k - k_0 \leq q \leq k + k_0 \\ 0 & \text{otherwise.} \end{cases}$$

The  $\mathbf{q}$ -vectors involved in the scattering process fill now the spherical shell  $V_S$  given by  $\Theta_q$  (Fig. 4). Partitioning the  $\mathbf{q}$ -integral into integrals over all BZ's  $V_\tau$  in  $V_S$  around reciprocal lattice vectors  $\boldsymbol{\tau}$  yields:

$$\bar{K} = C \sum_{\sigma} \sum_{\boldsymbol{\tau}} \int_{V_\tau} d\mathbf{q} \delta(\varepsilon - \hbar \omega^\sigma(\mathbf{q})) \cdot G^\sigma(\mathbf{q}). \quad (4a)$$

### 4. Bredov's Approximation

The decisive assumption of Bredov's approximation is that, whereas  $\delta(\varepsilon - \hbar \omega^\sigma(\mathbf{q}))$  is periodic in reciprocal

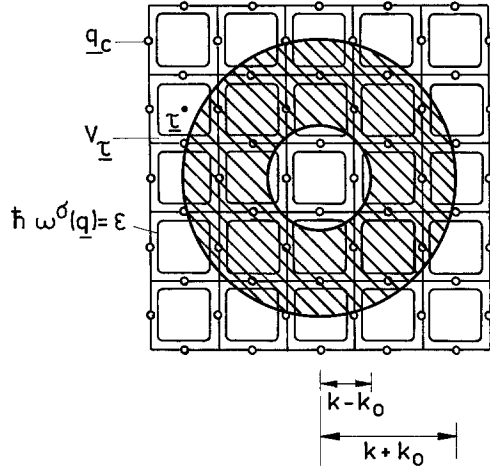


Fig. 4. Average over scattering angles (schematically): shaded area =  $\mathbf{q}$ -integration volume; one set of equivalent critical points,  $\mathbf{q}_c$ , is shown

space,  $G^\sigma(\mathbf{q})$  is slowly varying in  $V_\tau^*$  such that it can be replaced by its mean value  $\bar{G}_\tau$  averaged over  $\sigma$  and  $\mathbf{q}$  in  $V_\tau$ :

$$\bar{G}_\tau = 1/3 \cdot \sum_\sigma \cdot 1/V \int_{V_\tau} d\mathbf{q} G^\sigma(\mathbf{q})$$

and  $\bar{I}(\varepsilon)$  by

$$\begin{aligned} I_B(\varepsilon) &= \sum_\tau \bar{G}_\tau \sum_\sigma \int_{V_\tau} d\mathbf{q} \delta(\varepsilon - \hbar \omega^\sigma(\mathbf{q})) \\ &= \sum_\tau \bar{G}_\tau 3V g(\varepsilon) = g(\varepsilon) A(\varepsilon) \end{aligned} \quad (5)$$

$$A(\varepsilon) = 3V \sum_\tau \bar{G}_\tau = \int_{V_S} d\mathbf{q} q F(\mathbf{q})$$

( $\hbar \omega^\sigma(\mathbf{q})$  is periodic in reciprocal space). Consequently Bredov's assumption implies that  $g$  is approximately given by

$$g_B(\varepsilon) = \bar{I}(\varepsilon)/A(\varepsilon) \quad (6)$$

where  $\bar{I}(\varepsilon) = \bar{K}(\varepsilon)/C$  is directly measured and  $A(\varepsilon)$  can be calculated if  $F(\mathbf{q})$  is known; in the following we will always assume  $F \approx 1$ :

$$\begin{aligned} g_B(\varepsilon) &= \frac{C \sum_\sigma \int_{V_S} d\mathbf{q} \delta(\varepsilon - \hbar \omega^\sigma(\mathbf{q})) (\mathbf{q} \cdot \mathbf{e}^\sigma(\mathbf{q}))^2 \cdot 1/q}{C \sum_\sigma \int_{V_S} d\mathbf{q} (\mathbf{q} \cdot \mathbf{e}^\sigma(\mathbf{q}))^2 \cdot 1/q} \\ &= \frac{1}{8\pi k k_0 (k^2 + k_0^2)} \sum_\sigma \int_{V_S} d\mathbf{q} \delta(\varepsilon - \hbar \omega^\sigma(\mathbf{q})) \cdot (\mathbf{q} \cdot \mathbf{e}^\sigma(\mathbf{q}))^2 / q. \end{aligned} \quad (6a)$$

\* Strictly speaking this assumption only refers to the irreducible part of the BZ ( $1/48V$  for cubic crystals); this makes the assumption less restrictive, but for convenience here we refer to the whole BZ.

For practical applications this approximate spectrum  $g_B$  still has to be normalized (cp. Section 5b):  $g_B(\varepsilon) \rightarrow g_B(\varepsilon) / \int g_B(\varepsilon') d\varepsilon'$ .

## 5. The Accuracy of Bredov's Approximation

Generally the deviations of  $g_B$  from  $g$  arise for two reasons:

- polarization averaging:  $1/3 \cdot \sum_\sigma G^\sigma(\mathbf{q})$ ,
- $\mathbf{q}$ -averaging:  $1/V \cdot \int_{V_\tau} d\mathbf{q} G^\sigma(\mathbf{q})$ ,

the latter being dubious especially near the boundaries of  $V_S$ , where only parts of  $V_\tau$ 's are covered ("surface errors"). However, both approximations are justified well if many large  $\tau$ -vectors ( $\tau \gg V^{1/3}$ ) are involved; in this case polarization averaging is permitted for cubic crystals [1] and the "surface errors" are negligible. Consequently Bredov's approximation will become the more accurate the more one approaches the range of validity of the "incoherent approximation" [4] ( $k_0 \gg V^{1/3}$ )\*\*. To get a feeling of the errors involved we employ a nearest-neighbour-coupling model for a fcc lattice\*\*\* and compare two analytically calculated properties of the exact spectrum with those of  $g_B$ :

a) In 3-dimensional lattices the strongest singularities of  $g$  are of the square-root type at critical values  $\varepsilon_c$  where the first derivative becomes singular [8]:

$$g'(\varepsilon) = S(\varepsilon_c) \cdot (\varepsilon_c - \varepsilon)^{-1/2} \quad (\varepsilon \rightarrow \varepsilon_c - 0).$$

These singularities are caused by critical points  $\mathbf{q}_c$  in reciprocal space at which  $\text{grad}_{\mathbf{q}} \hbar \omega^\sigma(\mathbf{q}) = 0$ ,  $\hbar \omega^\sigma(\mathbf{q}_c) = \varepsilon_c$ ; both  $S(\varepsilon_c)$  and the corresponding Bredov-prefactor  $S_B(\varepsilon_c)$  can be calculated exactly [1]; they are determined by the immediate neighbourhood of  $\mathbf{q}_c$ , hence the deviation of  $S_B$  from  $S$  is mainly due to "surface errors": with increasing shell volume  $V_S$  there will be jumps in  $S_B$  whenever new critical points are collected by  $V_S$  (cp. Fig. 4). The example given in Fig. 5 refers to the longitudinal branch at the  $X$ -point (critical point by symmetry,  $\varepsilon_c = 41$  meV). The asymp-

\*\* The weight of very large  $\mathbf{q}$ -vectors is reduced by the DWF (for convenience we neglect the  $\mathbf{q}$ -dependence of the DWF, i.e. assume  $F(2\mathbf{k}_0) \approx 1$ , hence  $G^\sigma(\mathbf{q}) \sim q$ ). Further difficulties entering the determination of  $g$  from the "incoherent approximation" are resolution problems and multi-phonon processes.

\*\*\* The three force constants of this model can be fitted uniquely to the elastic constants [7]; therefore one obtains phonon dispersion curves, which by construction agree with experimental  $\omega^\sigma(\mathbf{q})$  for small  $q$ . Here we fit to the elastic data of Aluminium; in symmetry directions this model reproduces experimental dispersion curves with less than 10% error at the boundary of  $V$ . For the choice of the lattice model cp. Section 6. We chose Aluminium because Bredov's method was applied to it by several authors [2, 5].

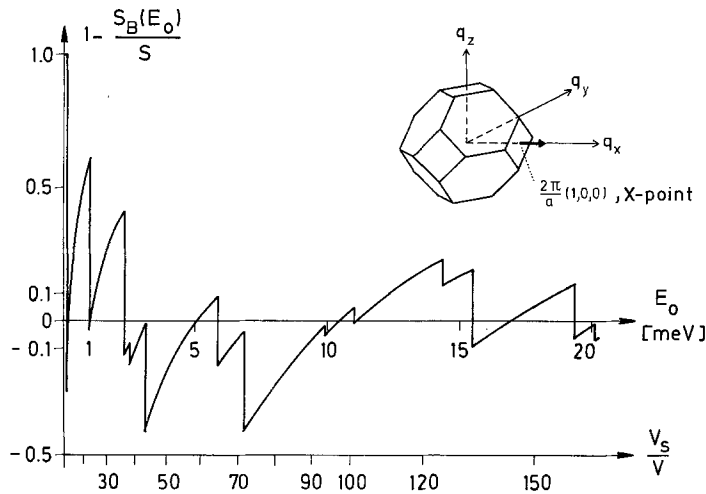


Fig. 5. Behaviour near van Hove singularities:  $g'_{(B)} = S_{(B)} \cdot (\epsilon_c - \epsilon)^{-1/2}$ , max. phonon energy ( $\epsilon_c = 41$  meV)

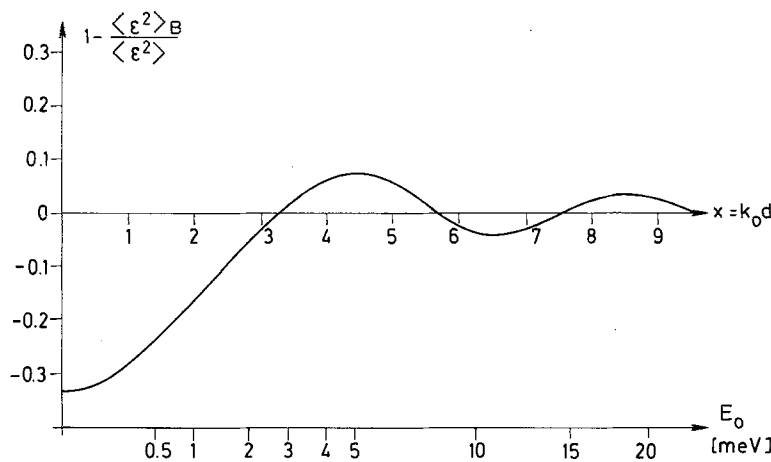


Fig. 6. Relative deviation of  $\langle \epsilon^2 \rangle_B$  from the exact value

total jump height (large  $k_0$ ) can be estimated roughly as  $\sim 1/(k_0 d) \sim (V/V_S)^{1/3}$  ( $d$ : nearest-neighbour distance) [1].

b) Whereas the behaviour near van Hove singularities refers to fixed  $\epsilon_c$  and is determined by points in reciprocal space, there are contributions from all phonon energies through the whole BZ to average values as  $\langle \epsilon^2 \rangle$ . The exact value can be obtained easily [7]; the corresponding Bredov average value,  $\langle \epsilon^2 \rangle_B = \int d\epsilon g_B(\epsilon) \epsilon^2$ , however, cannot be calculated in a straightforward way, since the  $q$ -integration boundaries  $k(\epsilon) \pm k_0$  entering  $\bar{I}(\epsilon)$  and  $A(\epsilon)$  explicitly depend on  $\epsilon^*$ . This difficulty can be circumvented if one replaces  $\epsilon$  in  $k(\epsilon)$  by a suitable mean value  $\tilde{\epsilon}$  (which implies the normalization of  $g_B$ ), e.g.  $\langle \epsilon^2 \rangle^{1/2}$  or  $\langle \epsilon^2 \rangle_B^{1/2}$ : in the latter case then  $\langle \epsilon^2 \rangle_B$  has to be

\* This furthermore implies that in general  $g_B(\epsilon)$  is not normalized.

determined self-consistently. The actual choice of  $\tilde{\epsilon}$ , however, does not affect  $\langle \epsilon^2 \rangle_B$  much if  $\tilde{\epsilon}$  is varied around  $\langle \epsilon^2 \rangle^{1/2}$  [1]. The relative deviation of  $\langle \epsilon^2 \rangle_B$  (self-consistently calculated) from  $\langle \epsilon^2 \rangle$  is shown in Fig. 6; asymptotically one has:  $-12 \cos(2k_0 d)/(2k_0 d)$ .

### 6. Conclusions

The results given in Section 5 are quite typical: they are confirmed by other examples\*\* (other averages and other van Hove singularities) discussed in detail in [1] which can be summarized as follows:

\*\* In [1] are treated furthermore:  $\langle \epsilon^2 \rangle_B$  with  $\tilde{\epsilon} = \langle \epsilon^2 \rangle^{1/2}$ ;  $\langle \epsilon^2 \rangle_B$ ,  $\langle \epsilon^4 \rangle_B$  and  $\int d\epsilon g_B(\epsilon)$  with  $\tilde{\epsilon} = 0$ , i.e.  $\epsilon_{max} \ll E_0$ ;  $\epsilon_c = 0$  (spectrum for small  $\epsilon$ ,  $g \sim \epsilon^2$ ): 100% error for  $E_0 \approx 5$  meV,  $\epsilon_c = 32$  meV (saddle point of the longitudinal branch in (110)-direction): 20% error for  $E_0 \approx 5$  meV.

a) The position of van Hove singularities is reproduced exactly including  $\varepsilon=0$  and  $\varepsilon=\varepsilon_{\max}$  (max. phonon energy).

b) The deviations of  $g_B(\varepsilon)$  from  $g$  depend on the incident neutron energy  $E_0$ . Both the integral ( $\langle\varepsilon^2\rangle_B$ ) and the specific ( $S_B(\varepsilon_c)$ ) properties of  $g_B$  display an oscillating behaviour around the exact results; in general  $g_B$  is not normalized.

c) For the indicated lattice model (maximum phonon energy 41 meV) and for cold incoming neutrons ( $E_0 \approx 5$  meV)  $g_B$  approximates  $g$  with respect to integral properties to about 5% and with respect to specific properties to about 50%.

Because roughly speaking Bredov's approximation is an averaging procedure in reciprocal space, it is obvious that  $g_B$  will describe those properties of  $g$  more reliably which do not refer to points or well localized regions but to larger parts of the BZ. This point of view furthermore allows to estimate the dependence of the results on the lattice model employed (nearest-neighbour-coupling, fitted to the small- $q$ -limit of experimental dispersion curves): a more realistic model including longer range coupling will introduce changes in  $\omega^\sigma(\mathbf{q})$  only for larger  $\mathbf{q}$ -vectors (in  $V$ ) such, that for higher  $\varepsilon$  the surfaces  $\hbar\omega^\sigma(\mathbf{q})=\varepsilon$  have a more complicated shape and extend over a larger region in the BZ; therefore for larger  $\varepsilon$  the errors in  $g_B$  arising from  $\mathbf{q}$ -averaging will be even smaller than those obtained from the nearest-neighbour-coupling model.

Consequently, the calculations given in this paper (and

in [1]) will describe fairly well the typical (maximum) deviations of Bredov's approximation from exact results and can serve as an estimate of its accuracy.

## References

1. Breuer, N.: On the determination of the phonon spectrum from coherent inelastic neutron scattering by polycrystals. Berichte der Kernforschungsanlage Jülich-Nr. 1035-FF, Jülich 1973
2. Bredov, M.M., Kotov, B.A., Okuneva, N.M., Oskotskii, V.S., Shakh-Budagov, A.L.: FTT 9, 287 (1967) (engl. transl.: Sov. Phys. Sol. St. 9, 214 (1967))
3. Oskotskii, V.S.: FTT 9, 550 (1967) (engl. transl.: Sov. Phys. Sol. St. 9, 420 (1967))
4. Turchin, V.F.: Slow Neutrons, Jerusalem: Israel Progr. for Scient. Transl. Ltd. 1965
5. Gompf, F., Lau, H., Reichardt, W., Salgado, J.: IAEA Sympos. on Neutron Inel. Scattering Report IAEA (SM-155) A-13, Grenoble (France) 1972  
isotropic  $\beta$ -distribution: Gompf, F., priv. comm.
6. Eremeev, I.P., Sadikov, I.P., Chernyshov, A.A.: FTT 15, 1953 (1973) (engl. transl.: Sov. Phys. Sol. St. 15, No. 7, 1309 (1974))
7. Leibfried, G.: Gittertheorie der mech. und therm. Eigenschaften der Kristalle. In: Encyclopedia of Physics, Vol. 7, Part 1. Berlin-Göttingen-Heidelberg: Springer 1955
8. Maradudin, A.A., Montroll, E.W., Weiss, G.H., Ipatova, I.P.: Theory of Lattice Dynamics in the Harmonic Approx. In: Sol. State Phys. Suppl. 3, 2nd ed. New York: Acad. Press 1971

Dr. N. Breuer  
Institut für Festkörperforschung  
der Kernforschungsanlage Jülich  
D-5170 Jülich 1  
Postfach 365  
Federal Republic of Germany